

## Ultrasonic attenuation and internal friction in $(\text{AgI})_x(\text{AgPO}_3)_{1-x}$ superionic glasses

R. Bogue\* and R. J. Sladek

*Department of Physics, Purdue University, West Lafayette, Indiana 47907*

(Received 5 March 1990; revised manuscript received 15 October 1990)

We have measured the attenuation of longitudinal and shear ultrasonic waves in  $(\text{AgI})_x(\text{AgPO}_3)_{1-x}$  glasses, with  $0 \leq x \leq 0.39$ , at temperatures between 80 and 360 K. We observe a large attenuation contribution, which increases with increasing frequency or AgI content. In samples with  $x \geq 0.31$ , this attenuation goes through a single broad peak as a function of temperature. The peak occurs at a higher temperature the greater the measuring frequency and its height increases with AgI content. These effects indicate that Ag-ion relaxation processes are involved. We fit our attenuation peaks and the internal friction peaks of Liu and Angell by using a modification of the "universal" relaxation function that Jonscher developed to account for non-Debye dielectric relaxation. From the fits we deduce relaxation activation enthalpies, exponents of the frequency-relaxation-time product, and relaxation amplitudes. We associate the activation enthalpies with potential barriers between alternative Ag sites, which may be affected by ion-ion correlation, discuss ways of accounting for the exponents, and account for the amplitudes by using different deformation potentials for Ag ions surrounded by oxide ions and for Ag ions surrounded by iodide ions, with both deformation potentials decreasing as AgI content increases.

### I. INTRODUCTION

Fast-ion conducting glasses have drawn substantial attention in recent years because of their possible use as solid electrolytes and the desire to understand how a disordered structure affects the fast ionic dynamics. Several studies have involved phosphate or borate glass systems containing AgI or LiI because of their high ionic conductivities, stability, and relative resistance to attack by moisture. These glasses can be readily prepared by quenching their melts to room temperature.

The system of  $(\text{AgI})_x(\text{AgPO}_3)_{1-x}$  glasses has been of particular interest. These glasses can be produced in a wide range of compositions ( $0 \leq x \leq 0.55$ ) without need for fast quenching techniques.<sup>1</sup> Rapid quenching extends this range up to 80% AgI.<sup>2</sup> Their ionic conductivity at room temperature is relatively high (e.g.,  $0.11 \Omega^{-1} \text{m}^{-1}$  for  $x=0.4$ ),<sup>3</sup> and can be further enhanced<sup>2</sup> by mixing with  $\text{B}_2\text{O}_3$ . Such mixed glasses have found commercial application as electrolytes in low current, long-shelf-life batteries.

Mechanical energy-loss measurements on  $(\text{AgI})_x(\text{AgPO}_3)_{1-x}$  glasses have hitherto involved low-frequency ( $\leq 110$  Hz) mechanical vibration measurements<sup>1</sup> or hypersonic (Brillouin) scattering of light.<sup>4</sup> These studies have revealed a non-Debye relaxation peak that is higher the greater the AgI content and becomes sharper at the highest frequencies.

We decided to investigate energy loss at ultrasonic frequencies to determine how it would compare with that in the other frequency ranges and to find a functional form to fit the loss peaks. As will be seen, our results are a natural extension of the low-frequency results but have the advantage of providing longitudinal as well as shear-wave losses.

From fitting a non-Debye relaxation to our shear-wave

results and/or the low-frequency mechanical-loss data of Liu and Angell, we deduce activation enthalpies, exponents of the frequency-relaxation time product, and deformation potentials.

### II. EXPERIMENT

#### A. Samples

Preparation of the  $(\text{AgI})_x(\text{AgPO}_3)_{1-x}$  samples used in this study has been described elsewhere.<sup>1,5</sup> The samples were 5–6-mm-thick clear disks, with a yellow tint that became more pronounced with increasing AgI concentration.

Upon inspection between crossed polarizers, all samples except the  $x=0.31$  sample showed roughly symmetric patterns that did not rotate when the sample was rotated. This might indicate either (i) radial internal strains or (ii) an average radial symmetry of  $\text{PO}_4$  chains in AgI-AgPO<sub>3</sub> glasses. We looked for any effect this apparent anisotropy might have on the shear modulus by measuring velocities and attenuations at 5 MHz with the polarization of the transducer aligned parallel, and then perpendicular, to a radial line. Different transducer orientations failed to show significant differences, assuring that effects due to anisotropy were below measurable limits.

#### B. Ultrasonic production and detection

Ultrasonic pulses were produced by applying 2–3- $\mu\text{s}$ -wide rf pulses from a Matec 6000 generator receiver to an X-cut or ac-cut quartz transducer attached to the sample. The ultrasound traveled to the far end of the sample where it was reflected for the return trip to the transducer, which converted some of each echo back into rf to be

amplified by the receiver section of the Matec unit. rf or video pulses from the receiver were displayed on an oscilloscope or sent to a Matec 2470 attenuation recorder, respectively.

Attenuation was measured directly from the height of the echoes displayed on the oscilloscope, or by the attenuation recorder, which would select two echoes by a gate and compare them in a logarithmic differential voltmeter circuit. Of the two methods, using the Matec 2470 was less tedious and normally capable of greater precision, but was prone to inaccuracy if the first echo was too small.

From room temperature down to about 180 K, Dow Corning 276-V9 resin served as a good bonding agent. A very small drop of the agent was placed on the sample face and heated with a blow dryer until the normally viscous resin flowed easily (about 60–80°C). The transducer was then placed on the sample and pressed down hard with a rubber eraser to squeeze out any excess resin. Achieving a thin, uniform bond was important. With practice, reasonable echoes could be obtained in about a third of the attempts.

Below 200 K, Dow Corning 200 fluid was used for both longitudinal and shear waves. It freezes to form a consistently high-quality bond that will support both shear and longitudinal waves with small loss, but may fail upon further cooling if the thermal expansion of sample, bond, and transducer differs significantly.

The sample, with attached transducer, was held by a spring-mounted sample holder and placed in an evacuable chamber within the liquid-nitrogen reservoir of a Dewar flask. By evacuating the chamber, the cooling rate could be held to less than 0.5°C/min, allowing data to be taken while cooling. Temperature was monitored by measuring the voltage drop across a calibrated platinum resistor carrying a constant 100  $\mu$ A current.

### C. Sources of extra attenuation

Once a good-quality bond is achieved, the measured attenuation still contains contributions besides that of primary interest (i.e., attenuation due to Ag-ion motion). These "extra" contributions are due to ordinary glassy relaxation processes<sup>6</sup> not associated with Ag-ion motion, diffraction of the ultrasonic waves,<sup>7</sup> and slight nonparallelism of the sample faces.<sup>7</sup> Since estimates of these contributions and that of the bond are of uncertain accuracy, we determined a background attenuation empirically from the attenuation data and used it to obtain results to be analyzed for Ag-ion relaxation effects.

## III. ULTRASONIC ATTENUATION

In  $\text{AgPO}_3$  glass we found that the attenuation<sup>8</sup> was generally similar to that in ordinary glasses so that instead of showing data plots for it we summarize our results as follows. The attenuation of 5 MHz longitudinal waves increased gradually with increasing temperature from  $0.16 \pm 0.01 \text{ cm}^{-1}$  at 197 K to  $0.20 \pm 0.01 \text{ cm}^{-1}$  at 296 K. The 5 MHz shear-wave attenuation also increased, rising from  $0.44 \pm 0.01 \text{ cm}^{-1}$  at 207 K to  $0.65 \pm 0.01 \text{ cm}^{-1}$

at 296 K. Above room temperature, the longitudinal-wave attenuation began to rise more steeply, reaching 0.43 at 360 K. This additional rise is attributed to the approach to the glass transition at 460 K.

The 15 MHz longitudinal- and shear-wave attenuations in  $\text{AgPO}_3$  were nearly three times those observed at 5 MHz in the more limited temperature range of the 15 MHz measurements.

The nearly linear frequency dependence and gradual rise with increasing temperature of the attenuation in  $\text{AgPO}_3$  glass are similar to those seen<sup>9</sup> in  $\text{As}_2\text{S}_3$  and other glasses, although the attenuation in  $\text{AgPO}_3$  glass is larger than in glasses not containing metal ions.

In contrast to our results on  $\text{AgPO}_3$  glass, we found that the attenuation of both longitudinal<sup>10</sup> and shear waves in  $(\text{AgI})_{0.31}(\text{AgPO}_3)_{0.69}$  glass went through a very broad peak centered near 290 K. The longitudinal-wave peak rose  $0.29 \text{ cm}^{-1}$  above a background attenuation of  $0.46 \text{ cm}^{-1}$ .

Our  $x = 0.39$  sample showed a large peak in both the 5 MHz longitudinal- and shear-wave attenuation, centered near 240 K, which shifted to 220 K when 2.35 MHz was used. (See Fig. 1 for shear-wave results.) No echoes were observable at 10 MHz or higher frequencies. The attenuation peak was larger for shear waves than for longitudinal waves. Both extended over a very broad temperature range.

Due to a large increase in the ultrasonic attenuation associated with the glass transition we could not discern a high-temperature peak like that reported by Angell and

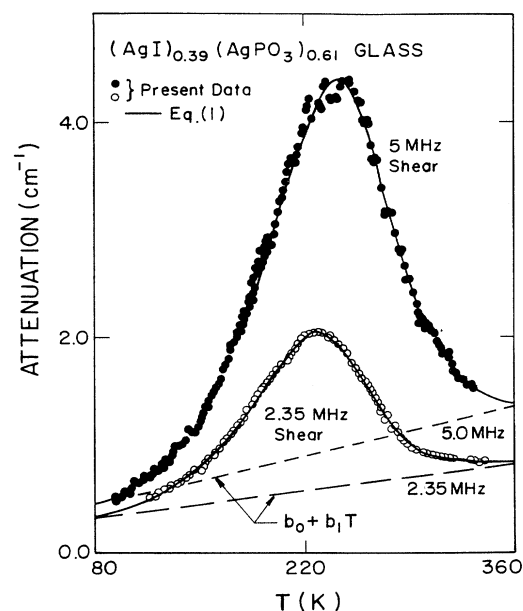


FIG. 1. Attenuation results obtained using 2.35 and 5.0 MHz shear waves in  $(\text{AgI})_{0.39}(\text{AgPO}_3)_{0.61}$  glass vs temperature. Results for  $x = 0$  and 0.31 are not shown to avoid clutter. The symbols give our experimental results. The curves were obtained by fitting Eq. (1) to the data as indicated in the text with the background attenuation  $b_0 + b_1 T$  given by the short-dashed line for 5 MHz and the long-dashed line for 2.35 MHz.

others at low frequencies for  $x=0$  and 0.2 glasses. The ultrasonic attenuation peak that we study corresponds to the low-temperature peak of Angell *et al.*, which has shifted to higher temperatures at our higher measuring frequencies.

Repeated measurements of the attenuation occasionally produced subsidiary minor peaks in the attenuation, superimposed on the main peak. These minor peaks<sup>10</sup> did not occur in all samples and could be made to disappear in a given sample by simply moving the transducer to another location on the sample face. The dependence on transducer location indicates that the minor peaks were due to small local fluctuations in the glass composition and, presumably, would not occur if the sample were completely homogeneous.

#### A. Modeling the Ag-ion relaxation

Relaxation effects in the ultrasonic attenuation of an elastic material are traditionally described in terms of the Debye model. A single Debye relaxation peak is too narrow<sup>11</sup> to fit either the observed mechanical or dielectric relaxation peak in  $(\text{AgI})_x(\text{AgPO}_3)_{1-x}$  glasses. This is not unusual for glasses. Indeed, many other materials also exhibit non-Debye relaxation effects.<sup>12,13</sup> Such behavior, which implies nonexponential relaxation in the time domain, is commonly explained in two different ways. One way involves using a sum of exponential relaxations characterized by a distribution of relaxation times  $w(\tau)$ . Such behavior is normally associated with a picture of *parallel* relaxation, in which each degree of freedom is allowed to relax independently. This yields a response function  $q(t) = q_0 \int_0^\infty w(\tau) e^{-t/\tau} d\tau$ . This method is conceptually simple, and can account for any reasonable  $q(t)$ , and its transform in the frequency domain, if the weight distribution  $w(\tau)$  is chosen suitably. It is often criticized, though, because  $w(\tau)$  is not understood in terms of microscopic processes.

The alternative way, which we will use, assumes that the relaxation behavior is nonexponential at the atomic level because of cooperative motion within a hierarchy of dynamical constraints. This is a *series* interpretation, in which the path to equilibrium involves many sequential correlated steps. Models of such many-body relaxations have been suggested by Jonscher,<sup>12,14</sup> Ngai and White,<sup>15</sup> and Palmer *et al.*<sup>16</sup>

We will summarize the work of Palmer *et al.*<sup>16</sup> as being especially illustrative. They have suggested a class of models for glassy relaxation under such hierarchically constrained dynamics, without providing any detailed mechanism. In their model, the fastest degrees of freedom might involve single-atom motion. Other atoms, or groups of atoms, might only be able to move appreciably when several of the fastest happen to move in just the right way, perhaps by leaving a vacancy or weakening a bond. Depending on assumptions made about the number of fast degrees of freedom needed to form a particular state before a slower degree of freedom may move, their models can predict either exponential ( $e^{-t}$ ), stretched exponential ( $e^{-t^\beta}$ ), or power-law ( $t^{-n}$ ) relaxation.

In the  $(\text{AgI})_x(\text{AgPO}_3)_{1-x}$  glass system the mobile Ag

ions are the fast movers, which we expect to be surrounded by oxide or by iodide ions, or by some combination thereof, in view of the structure of crystalline  $\text{AgPO}_3$  and the presence of AgI regions within the glass. (More will be said about this later.) The iodide cage in the AgI regions and the oxide cage comprised of oxide ions in three different phosphate chains will shift in response to Ag-ion motion via rapid modes since slower modes will be suppressed by new silvers occupying the vacated Ag sites. However, when particular Ag configurations are attained, slower iodide and phosphate movements may occur.

We found general expressions that were capable of describing both our own data and also the low-frequency mechanical  $\tan\delta$  ( $=Y''/Y'$ , where  $Y=Y'+iY''$  is the complex Young modulus) results of Liu and Angell (see Fig. 2). The relation fitting our ultrasonic data combined a background attenuation that rose linearly with increasing  $T$  with slightly modified Jonscher "universal" relaxation function, as adapted by Almond and West<sup>17,18</sup> to describe Na-ion relaxation in  $\beta$ -alumina. Following Almond and West, we used a single characteristic relaxation time  $\tau$ , rather than the two times used in Jonscher's original expression. The attenuation relation is

$$\alpha = b_0 + b_1 T + \frac{A\omega}{2vT} [(\omega\tau)^{-m} + (\omega\tau)^{1-n}]^{-1}, \quad (1)$$

where  $v$  is the ultrasonic wave velocity and  $\tau = \tau_0 e^{E_a/kT}$ . The constant  $b_0$  includes any background attenuation

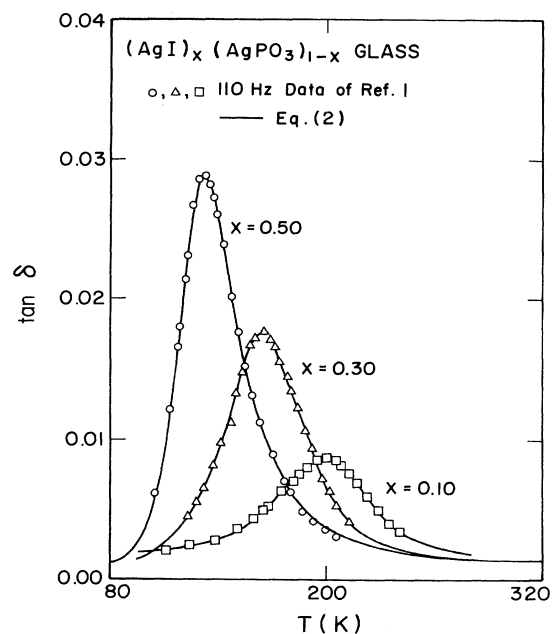


FIG. 2. Mechanical energy loss in  $(\text{AgI})_x(\text{AgPO}_3)_{1-x}$  glasses at 110 Hz. Results are shown for only three concentrations to avoid clutter. The symbols give data from Ref. 1. The curves were obtained by fitting Eq. (2) to the data as indicated in the text with  $\delta_0 = 0.0020, 0.0012, \text{ and } 0.0011$  at  $x = 0.1, 0.3, \text{ and } 0.5$ , respectively, and  $\delta_1 = 0$  for all three concentrations.

due to diffraction and bond effects, the diffraction contribution varying inversely with ultrasonic frequency.<sup>7</sup> We attribute the  $b_1 T$  term mainly to "ordinary" glassy relaxation processes, which, in view of data on nonsuperionic glasses, we expect to increase nearly linearly with frequency.

The analogous expression for the mechanical relaxation  $\tan\delta$  is

$$\tan\delta = \delta_0 + \delta_1 T + \frac{A}{T} [(\omega\tau)^{-m} + (\omega\tau)^{1-n}]^{-1}. \quad (2)$$

Because the  $\tan\delta$  measurements were performed at lower temperatures than the ultrasonic attenuation measurements, the  $\delta_1 T$  term in the background was very small in all but the  $x=0$  sample. It was set equal to zero during the curve fitting process.

In order to account for the effects of temperature on the relaxation strength, the third term in Eqs. (1) and (2) includes a  $1/T$  factor that is based on Jackle's theory<sup>19</sup> for relaxation due to motion of ions between alternative positions representable by a double potential well. Later we shall also use ideas from Jackle's theory to account for the amplitude factor  $A$ .

Before discussing the exponents and relaxation time in Eqs. (1) and (2), we would like to point out that the reason we have used the Jonscher-based relaxation term is that it fits internal friction data much better than does a form based on a stretched exponential  $e^{-(t/\tau)^\beta}$  in which  $\beta$  is independent of temperature. The Appendix contains a figure showing fits of internal friction data achieved using the Jonscher-based form and a stretched exponential-based form. We have not tried using a two-exponent-containing expression based on the Havriliak-Negami function  $[1 + (i\omega\tau)^{1-\alpha}]^{-\beta}$ , which is useful for fitting the frequency dependence of dielectric relaxation in polymers, because those authors found that their  $\alpha$  and  $\beta$ , as well as  $\tau$ , had to vary with temperature in order to fit experimental results.<sup>20</sup> In contrast, our fits are achieved without this complication, i.e., our exponents do not depend on temperature.

Jonscher's analysis<sup>14</sup> for dielectric relaxation via *tunneling* interprets the exponents  $m$  and  $1-n$  in terms of the behavior of correlated two-level systems having a range of energies. The precise form of the distribution of system energies is not critical to his analysis, but he gives it a characteristic width  $2\xi$ . If the typical switching potential due to the abrupt dipolar or charge-carrier "flip" from one minimum of a double potential well to the other is  $V_f$ , then the low-temperature exponent  $1-n$  in the Jonscher relation has  $n = |V_f/2\xi|^2$ .

Similarly, if the average switching potential for two neighboring two-level systems to have two ions shift in opposite senses is  $V_{ff}$ ; the high-temperature exponent  $m$  is given by  $m = |V_{ff}/2\xi|^2$ , where  $2\xi$  is the maximum energy spread of these "flip-flop" associated transitions. When the relaxation time  $\tau$  is sufficiently short, these latter transitions do not have time to intervene. In this case, the limiting low-frequency response is proportional to  $\omega$ , i.e.,  $m=1$ .

Whether or not the Jonscher function actually represents some type of microscopic physical process is

not known, although the Palmer *et al.* description can yield Jonscher's power-law relaxations, and Dissado and Hill<sup>13</sup> attempt to make such a representation. We have used the Jonscher function because it enables us to fit an entire peak remarkably well with a single relaxation function involving a single relaxation time plus background terms.

Because of not having data at enough different frequencies to determine  $\tau_0$  and  $E_a$  independently, we chose  $\tau_0 = 4.61 \times 10^{-14}$  sec corresponding to the  $115 \text{ cm}^{-1}$  Ag-I Raman mode<sup>21</sup> to fit both our ultrasonic attenuation results and the 110 Hz internal friction data of Liu and Angell. [Use of a  $\tau_0$  value for  $\text{AgPO}_3$  derived from the  $60 \text{ cm}^{-1}$  Ag-O mode yielded about the same values for the parameters in Eq. (2) as did the  $\tau_0$  value obtained from the  $115 \text{ cm}^{-1}$  Ag-I mode, so the latter was used for all samples.] The  $E_a$  values we found by fitting our ultrasonic data and the Liu and Angell  $\tan\delta$  data are plotted in Fig. 3. It can be seen that the  $E_a$  values from both sets of data agree and that  $E_a \approx (0.49 \text{ eV})(1 - 0.81x)$ , where  $x$  is the fractional AgI content. Extrapolation to  $x=1$  gives 0.093 eV for pure AgI in excellent agreement with the value of 0.095 eV for crystalline  $\alpha$ -AgI.<sup>22</sup> The  $E_a$ 's we associate with potential barriers between alternative Ag sites although we have not been able to develop a model that can account for their values. Furthermore, ion-ion correlations might result in the observed activation enthalpies not being associated with barriers to one body motion. For example, Ngai *et al.* found<sup>23</sup> that the nuclear spin-relaxation energy for some  $(\text{Na}_2\text{O})_x(\text{GeO}_2)_{1-x}$  glasses is about equal to  $\beta$  times the conductivity activation energy where  $\beta$  is the exponent in the Kohlrausch-Williams-Watts<sup>24</sup> stretched exponential relaxation function  $e^{-(t/\tau)^\beta}$ . Thus they suggest that the conductivity relaxation energy does not equal the microscopic barrier between two adjacent wells because of ion-ion correlation

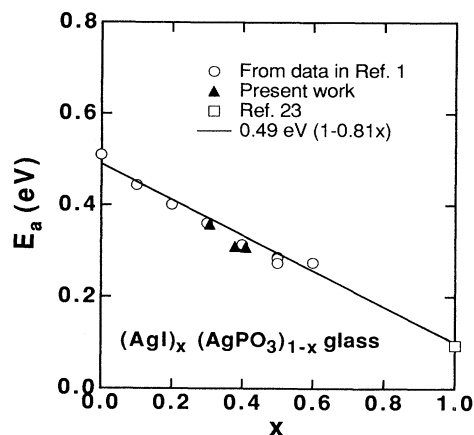


FIG. 3. Relaxation rate activation enthalpy for various  $(\text{AgI})_x(\text{AgPO}_3)_{1-x}$  glasses and for the  $\alpha$ -AgI crystal at  $x=1$ . We deduced the values for the glasses from 5.0 MHz ultrasonic attenuation data (present work) and 110 Hz mechanical loss data (Ref. 1). The  $\alpha$ -AgI value was taken from Ref. 23. The line represents the best fit to these data.

(which is indicated by  $1-\beta$  not being zero.) Whether or not analogous concepts are relevant to the interpretation of our  $E_a$  values is not known. It should be noted that our  $E_a$  values are equal, to within experimental error, to those obtained from the electric modulus or conductivity<sup>3</sup> of samples from the same source (Liu and Angell) as ours. The fact that the mechanical-loss peak is wider than the dielectric-loss peak (as found in Ref. 1) implies that although Ag ions are involved in both types of relaxation, mechanical loss must also involve motion of some nonpolar entities comprised of a Ag ion and some of its surrounding ions. Such motion would be consistent with that responsible for the Ag-I Raman mode whose frequency we have used in our analysis.

From our fits to the 110 Hz measurements of Liu and Angell, we find that the high-temperature (low-frequency) exponent  $m$  decreases with increasing AgI content from 0.63 at  $x=0.1$  to 0.32 at  $x=0.5$  before rising again to 0.41 at  $x=0.6$ . A value of  $m$  is difficult to obtain for the  $x=0$  sample because the character of the background loss changes at that temperature from essentially constant to rapidly increasing as the high-temperature peak is approached. A good estimate for  $m$  at  $x=0$  would be about 1.3.

At the same time, the low-temperature (high-frequency) Jonscher exponent  $1-n$  falls slightly from 0.29 at  $x=0$  to 0.21 at  $x=0.2$  before rising to 0.43 at  $x=0.5$  and 0.41 at  $x=0.6$ .

The exponents  $m$  and  $1-n$  are quite different for AgI content less than 30% but very nearly equal at AgI concentrations of 50% and 60%. The high values of  $m$  for low AgI content suggest a change in the degree of localization such that only back and forth hopping occurs at low concentrations, while consecutive hops can occur above a percolation threshold at  $x=0.3$ .

Using 5 MHz shear waves, the high-temperature exponent  $m$  falls from 1.23 at  $x=0.31$  to 0.88 at  $x=0.39$ . The low-temperature exponent  $1-n$  falls slightly from 0.28 at  $x=0.31$  to 0.26 at  $x=0.39$ .

Jonscher says that, for dielectric relaxation, sharpening of the peak corresponding to an increase in  $m$  and a decrease in  $n$  as  $T$  increases is understandable in terms of more structural disorder reducing the correlation flip transitions but increasing the correlation of flip-flop transitions.

The values of the amplitude factor  $A$  obtained by fitting Eq. (2) to the Liu and Angell data are shown in Fig. 4. They satisfy the empirical expression  $A=(0.60+10.66x^{0.71})$  K, where  $x$  is the fractional AgI content. Although seemingly peculiar, this form for  $A$  can be explained in terms of the energy loss due to hysteretic hopping of Ag ions between alternative sites as a consequence of elastic wave modulation of the energy difference between the sites. The structure of the glasses allows two kinds of alternative site systems.

One type of alternative site system is associated with the silver ions between chains of  $\text{PO}_4^-$  tetrahedra in  $(\text{AgI})_x(\text{AgPO}_3)_{1-x}$  glasses. This system was inferred from the fact that five oxide ions surround each Ag ion in crystalline  $\text{AgPO}_3$ . In view of the small density of tunneling states in most glasses, only a certain fraction,  $f$ , of the

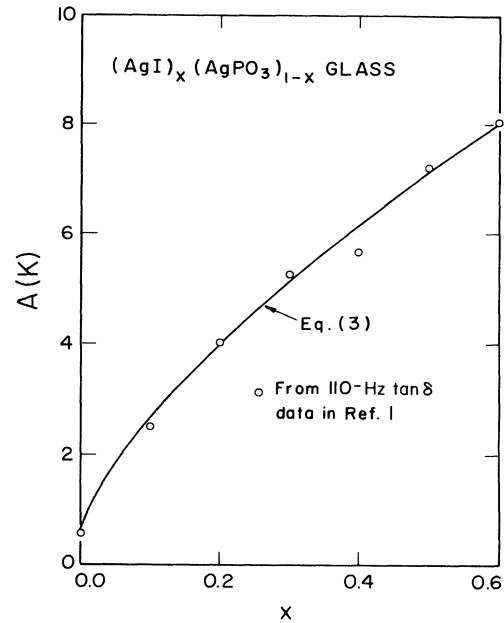


FIG. 4. Silver-ion relaxation amplitude factor in  $(\text{AgI})_x(\text{AgPO}_3)_{1-x}$  glasses at 110 Hz. Symbols give  $A$  values determined by fitting Eq. (2) to data from Ref. 1. The curve shows how Eq. (3) can fit the  $A$  values when the Ag-I deformation-potential values are chosen appropriately (see text).

oxide-surrounded silvers are likely to contribute to mechanical energy loss. Elastic wave modulation of the energy difference between the alternative Ag sites in this environment will be represented by means of a deformation potential  $D_{\text{Ag-O}}$ .

Another type of alternative site system is due to regions of AgI in  $(\text{AgI})_x(\text{AgPO}_3)_{1-x}$  glasses, which are similar in local order to that of crystalline  $\alpha$ -AgI. Within these regions the silver ions are surrounded mainly by iodide ions. Essentially all of these silvers contribute to mechanical energy loss. These sites are analogous to the tetrahedral Ag-ion sites within the bcc iodide ion lattice of  $\alpha$ -AgI. Elastic wave modulation of the energy difference between alternative iodide-surrounded Ag sites will be represented by means of a deformation potential  $D_{\text{Ag-I}}$ . Essentially all iodide-surrounded silvers are thought to contribute to mechanical energy loss in the present glass system because essentially all silvers seem to be mobile in  $\alpha$ -AgI, as inferred from electrical conductivity and EXAFS measurements,<sup>25</sup> and molecular-dynamics calculations.<sup>22</sup>

An expression for  $A$  based on the above considerations is

$$A = \frac{(N/V)_{\text{Ag}}[(1-x)fD_{\text{Ag-O}}^2 + xD_{\text{Ag-I}}^2]}{2k_B Y}, \quad (3)$$

where  $(N/V)_{\text{Ag}}$  is the number of silvers per unit volume equal to  $1.43 \times 10^{22}(1+0.15x) \text{ cm}^{-3}$ ,  $k_B$  is Boltzmann's constant, and  $Y$  is Young's modulus  $[=3BC_T/(B + \frac{1}{3}C_T) = 2.73 \times 10^{11}(1-0.845x) \text{ d/cm}^2]$ , which is ap-

propriate for the internal friction data. (For  $A$  obtained from ultrasonic shear-wave attenuation,  $Y$  would be replaced by the shear modulus,  $C_T$ .)

Before proceeding further, it is appropriate to note that neither this expression for  $A$ , nor the preceding discussion, takes explicit account of the possibility of energy loss due to Ag ions moving at the interface between the AgI regions and the  $\text{PO}_4^-$  chains. This was not done because such a contribution is thought either to be negligible and/or to be taken care of by the fact that  $D_{\text{Ag-O}}$  and  $D_{\text{Ag-I}}$  seem to depend on AgI and  $\text{AgPO}_3$  contents for the reasons given below.

We obtain values for  $D_{\text{Ag-O}}$  by using an empirical relation for covalent glasses<sup>26</sup> that connects the deformation potential to the glass temperature,  $T_g$ , i.e.,  $D_{\text{Ag-O}} = 8.12 \times 10^{-4} T_g$  eV. Since in the present glass system  $T_g \approx 460(1 - 0.43x)$  K, then  $D_{\text{Ag-O}} = 0.372(1 - 0.43x)$  eV. Using the experimental values of  $A$ ,  $Y$ , and  $(N/V)_{\text{Ag}}$  for  $x=0$ , along with  $D_{\text{Ag-O}} = 0.372$  eV for  $x=0$ , yields a value for  $f$  of  $8.9 \times 10^{-3}$ . The reasonableness of this value can be seen by using it to calculate a density of states for comparison with the density of low-temperature tunneling states in various glasses. Dividing  $(N/V)_{\text{Ag}} f$  by the maximum reasonable range of energy states,  $k_B T_g$ , one obtains  $2 \times 10^{33} \text{ erg}^{-1} \text{ cm}^{-3}$ . In comparison, a value of  $2 \times 10^{32} \text{ erg}^{-1} \text{ cm}^{-3}$  has been found for covalent glass<sup>26</sup> of comparable  $T_g$  and a value of  $1 \times 10^{33} \text{ erg}^{-1} \text{ cm}^{-3}$  for  $(\text{B}_2\text{O}_3)(\text{Li}_2\text{O})_{0.5}(\text{LiCl})_{0.7}$  superionic glass.<sup>27</sup> All these densities of states imply tunneling site concentrations that are much smaller than the ionic concentrations.<sup>28,29</sup>

Assuming that the fraction of oxide-surrounded silvers that contribute to mechanical energy loss is independent of concentration, we proceed by requiring Eq. (3) to fit experimental values of  $A$  for  $x > 0$  [using appropriate values for  $(N/V)_{\text{Ag}}$  and  $Y$  of course]. This yields  $D_{\text{Ag-I}} \approx 0.22(1 - 0.88x)$  eV. Thus,  $D_{\text{Ag-I}}$  decreases more rapidly with increasing AgI content than if it were proportional to the glass temperature, since  $T_g \sim (1 - 0.43x)$  as mentioned above. Extrapolation of the above expression for  $D_{\text{Ag-I}}$  to  $x=1$  yields  $D_{\text{Ag-I}} = 0.026$  eV, which would imply very small phonon-Ag-ion coupling and relaxational elastic energy loss due to Ag motion in AgI.

#### IV. SUMMARY

We have made a determination of mechanical energy loss at ultrasonic frequencies for  $(\text{AgI})_x(\text{AgPO}_3)_{1-x}$  glasses, with  $0 \leq x \leq 0.39$ .

Ultrasonic attenuation data of ours and low-frequency mechanical-loss data of Liu and Angell in  $(\text{AgI})_x(\text{AgPO}_3)_{1-x}$  glasses have large contributions due to relaxation processes that are consistent with thermal activation of Ag ions between alternative sites describable by a Jonscher "universal" relaxation function. The activation energies (actually enthalpies) determined at our ultrasonic frequencies are very close to those determined at 110 Hz by Liu and Angell for comparable AgI concentrations and to those obtained from electrical measurements by Mangion and Johari using samples provided by Liu and Angell (as were ours). This confirms that the use

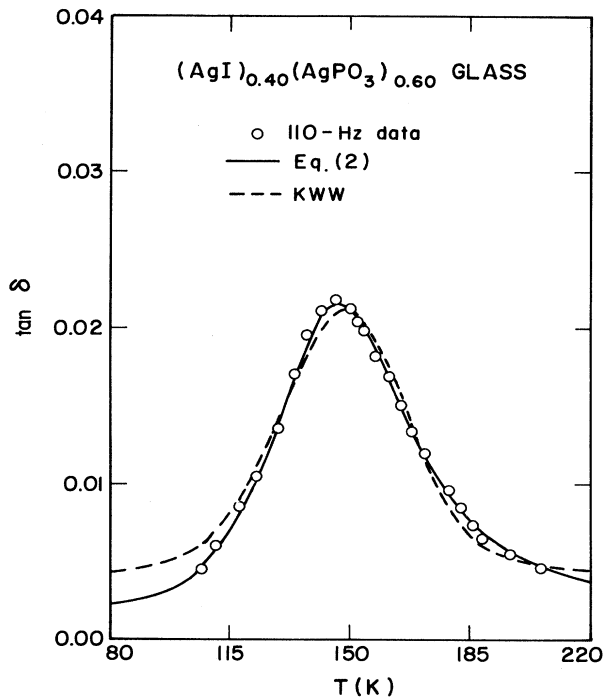


FIG. 5. Internal friction vs temperature data in  $(\text{AgI})_{0.40}(\text{AgPO}_3)_{0.60}$  glass and curves calculated to fit the data. The dashed KWW curve was derived for a time domain relaxation of  $e^{-(t/\tau)^\beta}$ , where  $\beta=0.36$  and  $\tau=\tau_0 e^{E_a/kT}$  with  $E_a=0.310$  eV. The solid Eq. (2) curve was calculated using  $m=0.37$ ,  $1-n=0.31$ , and  $\tau=\tau_0 e^{E_a/kT}$  with  $E_a=0.310$  eV. For both calculated curves  $\tau_0=4.61 \times 10^{-14}$  s.

of an Arrhenius form for the relaxation time is appropriate over a frequency span of five orders of magnitude. The high- and low-temperature Jonscher exponents of the frequency-relaxation-time product in the Jonscher function  $m$  and  $1-n$ , respectively, are different for the two frequency ranges, indicating that cooperative relaxation effects are either temperature and/or frequency dependent.

The amplitude of the silver-ion relaxation can be interpreted in terms of strain-induced shifts of energy levels involving a weighted sum of the squares of two deformation potentials. Values of the deformation potential for the relaxation of silvers in an oxide environment ( $D_{\text{Ag-O}}$ ) were estimated from the glass temperature and thus decreased as AgI content increased. The other deformation potential ( $D_{\text{Ag-I}}$ ), for the relaxation of silvers in an iodide environment, decreased about twice as strongly with increasing AgI content as did  $D_{\text{Ag-O}}$ . This is consistent with cooperative relaxation in the iodide-rich regions, as the silver-phonon coupling would be affected by changes in the environment of neighboring silvers.

#### ACKNOWLEDGMENTS

Thanks are due to Professor C. A. Angell and C. L. Liu for the samples used in this study, the use of their

data in our analyses, and for many helpful discussions, and to Dr. C. Guerra-Vela and Dr. P. Maheswaranathan for help with the ultrasonic apparatus. The initial part of this work was supported in part by the National Science Foundation via Grant No. DMR79-08538A3 and the Materials Research Laboratory Program Grant No. DMR83-16988.

#### APPENDIX

The ultrasonic attenuation we measured and the low-frequency internal friction in Ref. 1 for  $(\text{AgI})_x(\text{AgPO}_3)_{1-x}$  glasses each exhibits a relaxation

peak as a function of temperature, which we found is well fitted by an expression having a term containing the Jonscher function  $[(\omega\tau)^{-m} + (\omega\tau)^{1-n}]^{-1}$  divided by temperature as indicated in the body of this paper. Many investigators have tried to fit non-Debye relaxations with an expression based on the Kohlrausch-Williams-Watts (KWW) stretched exponential  $e^{-(t/\tau)^\beta}$  in which  $\tau$  is the relaxation time and  $\beta < 1$ , and indeed Liu and Angell<sup>1</sup> made such an attempt to fit their internal friction data. Therefore we present Fig. 5 to show that the KWW form does not fit internal friction data as well as the expression that we have employed in this work.

\*Present address: Department of Physics, Illinois State University, Normal, IL 61761.

<sup>1</sup>C. Liu and C. A. Angell, *J. Non-Cryst. Solids* **83**, 162 (1986).

<sup>2</sup>S. Radhakrishna (private communication).

<sup>3</sup>M. B. M. Mangion and G. P. Johari, *Phys. Chem. Glass* **29**, 225 (1988).

<sup>4</sup>L. Börjesson, S. W. Martin, L. M. Torell, and C. A. Angell, *Solid State Ion.* **18&19**, 141 (1986).

<sup>5</sup>R. Bogue and R. J. Sladek, *Phys. Rev. B* **42**, 5280 (1990).

<sup>6</sup>S. Hunklinger and W. Arnold, in *Physical Acoustics, Vol. XII*, edited by W. P. Mason and R. N. Thurston (Academic, New York, 1976), p. 155.

<sup>7</sup>R. Truell, C. Elbaum, and B. Chick, *Ultrasonic Methods in Solid State Physics* (Academic, New York, 1969), p. 161ff and Appendix H.

<sup>8</sup>R. Bogue, Ph.D. thesis, Purdue University, 1989.

<sup>9</sup>D. Ng and R. J. Sladek, *Phys. Rev. B* **11**, 4017 (1975).

<sup>10</sup>R. Bogue, R. J. Sladek, and C. Liu, *J. Phys. (Paris) Colloq.* **46**, C10-489 (1985).

<sup>11</sup>C. Liu and C. A. Angell, *J. Phys. (Paris) Colloq.* **46**, C10-493 (1985).

<sup>12</sup>A. K. Jonscher, *Nature* **267**, 673 (1977).

<sup>13</sup>L. A. Dissado and R. M. Hill, *Nature* **279**, 685 (1979).

<sup>14</sup>A. K. Jonscher, in *Physics of Dielectric Solids*, Inst. Phys. Conf. Ser. No. 58, edited by C. H. L. Goodman (IOP, Bristol,

1980), p. 22.

<sup>15</sup>K. L. Ngai and C. T. White, *Phys. Rev. B* **20**, 2475 (1979).

<sup>16</sup>R. G. Palmer, D. L. Stein, E. Abrahams, and P. W. Anderson, *Phys. Rev. Lett.* **53**, 958 (1984).

<sup>17</sup>D. P. Almond and A. R. West, *Phys. Rev. Lett.* **47**, 431 (1981).

<sup>18</sup>D. P. Almond, G. K. Duncan, and A. R. West, *J. Non-Cryst. Solids* **74**, 285 (1985).

<sup>19</sup>J. Jackle, *Z. Phys.* **257**, 212 (1972).

<sup>20</sup>S. Havriliak and S. Negami, *J. Polymer Sci. C* **14**, 99 (1966).

<sup>21</sup>J. P. Malugani and R. Mercier, *Solid State Ion.* **13**, 293 (1984).

<sup>22</sup>P. Vashista and A. Rahman, *Phys. Rev. Lett.* **40**, 1337 (1978).

<sup>23</sup>K. L. Ngai, J. N. Moody, H. Jain, O. Kanert, and G. Balzer-Jollenbeck, *Phys. Rev. B* **39**, 6169 (1989).

<sup>24</sup>M. Dishon, G. H. Weiss, and J. T. Bendler, *J. Res. Nat. Bur. Stand.* **90**, 27 (1985).

<sup>25</sup>J. B. Boyce, T. M. Hayes, W. Stutius, and J. C. Mikkelsen, Jr., *Phys. Rev. Lett.* **38**, 1362 (1977).

<sup>26</sup>U. Reichert, M. Schmidt, and S. Hunklinger, *Solid State Commun.* **57**, 315 (1986).

<sup>27</sup>J. Y. Prieur and D. Čiplys, *Physica B+C* **107B**, 181 (1981).

<sup>28</sup>M. H. Cohen and G. S. Grest, *Phys. Rev. Lett.* **45**, 1271 (1980).

<sup>29</sup>M. H. Cohen and G. S. Grest, *Solid State Commun.* **39**, 143 (1981).